Journal of Cardiovascular Translational Research (2022) 15:1393–1405
https://doi.org/10.1007/s12265-022-10267-4

ORIGINAL ARTICLE

Circulating exosome-derived miR-122-5p is a novel biomarker for prediction of postoperative atrial fibrillation

Chen Bai[1] · Yisi Liu[2] · Yichen Zhao[1] · Qing Ye[1] · Cheng Zhao[1] · Yang Liu[1] · Jiangang Wang[1]

Received: 15 March 2022 / Accepted: 21 April 2022 / Published online: 5 May 2022

Abstract

Postoperative atrial fibrillation (POAF) is a frequent complication associated with increased periprocedural mortality and morbidity after cardiac surgery. Our study aimed to identify the difference in exosomal miRNA and further explore its role in the diagnosis of POAF. First, the differentially expressed miRNAs (DEMs) were obtained by high-throughput RNA sequencing. Second, the DEMs target genes were put into gene ontology (GO) and KEGG pathway analysis. Third, real-time quantification PCR (RT-qPCR) was used to verify the DEMs. Finally, we revealed 23 DEMs in POAF patients. Furthermore, analysis of gene function revealed that DEMs may affect atrial structure through many signaling pathways. We also found that miR-122-5p was up-regulated in POAF patients, but there are no significant changes in miR-191-5p, miR-181a-5p, miR-155-5p and miR-151a-5p. Our study revealed that exosomal miRNAs exert enormous potential in evaluating the severity or prognostic of POAF.

Keywords Postoperative atrial fibrillation (POAF) · Exosomes · High-throughput RNA sequencing · microRNA (miRNA)

Introduction

New-onset postoperative atrial fibrillation (POAF) is a frequent complication following approximately 18–57% of cardiac surgery [1, 2], which has a well-documented negative impact on coronary artery bypass grafting surgery (CABG) [3, 4]. POAF is associated with increased perioperative mortality and morbidity, increased expenses, prolonged hospital stays, and decreased long-term survival [5, 6]. However, current POAF diagnostic methods, twelve lead electrocardiography and ambulatory electrocardiographic recording devices are not very efficient [7, 8]. Therefore, the development of more convenient and effective diagnostic tools is of great value for the early diagnosis and prevention of POAF. New insights into the pathogenesis of POAF will contribute to the development of clinical biomarkers [9]. Recent studies suggest that circulating microRNAs (miRNAs) serve as potential diagnostic biomarkers for cardiovascular disease [10, 11], although some studies have shown that cardiomyocyte-derived miRNAs may be involved in cardiomyocyte metabolism and remodeling [12, 13]. However, the role of circulating exosomal miRNAs in the pathophysiology of POAF has been poorly studied.

Exosomes are the smallest (diameters ranging from 30 to 200 nm) endogenous extracellular vesicles (EVs) that exist inside multi-vesicles due to endosome compartmentalization [14]. Exosomes contain many biologically active substances, such as lipids, proteins, DNAs, mRNAs, and cell-derived miRNA [15]. Among these substances, miRNAs can reduce gene expression by degrading or inhibiting target mRNAs, thereby further regulating various biological pathways involved in target genes [16]. Multiple studies have also shown that non-parent cells that take up exosomal miRNAs can act as intercellular messengers in local and long-range micro-communication mechanisms [17]. Exosomal miRNAs can be produced in a biologically active form by parent cells and are not cleared in biological fluids, showing their potential as novel biomarkers [18]. Previous studies have shown a close association between exosomes and cardiovascular disease [19]. However, its role in the development of POAF remains unknown.

Associate Editor Junjie Xiao oversaw the review of this article.

✉ Jiangang Wang
jiangangwang@ccmu.edu.cn

[1] Department of Cardiovascular Surgery, Beijing Anzhen Hospital, Capital Medical University, Beijing 100029, China

[2] School of Nursing, Capital Medical University, Beijing 100069, China

In this study, we aimed to identify differences in exosomal miRNAs in POAF patients using a high-throughput sequencing approach to explore possible mechanisms of POAF progression. Then, the relative levels of differential expression of exosomal miRNAs in POAF and non-POAF patients were verified by the real-time PCR method. These findings can help identify the underlying mechanisms of POAF and help develop more promising therapeutic targets.

Material and Methods

Patient recruitment and specimen collection

This study enrolled patients who underwent elective coronary artery bypass grafting (CABG) surgery in the Department of Cardiac Surgery, Beijing Anzhen Hospital (Beijing, China), between May 2019 and June 2020. Participants were aged 18–90 years, without heart failure (HF) or atrial fibrillation (AF), preserved left ventricular function, and undergoing CABG as elective surgery only. POAF was defined as a new-onset irregular rhythm with no apparent P waves lasting at least 30 s, detected in patients by telemetry-based continuous electrocardiographic (ECG) monitoring or 12-lead ECG during hospitalization. A total of 6 POAF patients and 6 non-POAF patients were selected in the miRNA sequencing step, and a total of 10 POAF patients and 10 non-POAF patients were selected in the validation step. The clinical characteristics of the patients were obtained from the medical record system (Table 1 and Table 2).

Whole blood samples were obtained from all participants 24 h before surgery and in the morning before breakfast, and plasma was extracted from whole blood by centrifugation at 3000 × g for 15 min and stored at − 80 °C before exosome extraction. All procedures performed in this study were approved by the Ethics Committee of Beijing Anzhen Hospital, and informed consent was obtained from all individuals involved in this study or their guardians.

Isolation of plasma exosomes

Plasma samples were thawed at 37 ℃ and centrifuged at 3000 × g for 15 min to remove cells and debris. The supernatant was then diluted with 7 times the volume of PBS, followed by centrifugation at 13,000 × g for 30 min, and the large particles were removed using a 0.22-μm filter membrane. The supernatant was centrifuged with the P50A72-986 rotor (CP100NX; Hitachi, Brea, CA, USA) at 4 ℃ 100,000 × g for 2 h to obtain the exosome pellet and then repeated the centrifugation process after the pellet was resuspended with PBS. Finally, 100 μl PBS was added to resuspend the pellet to obtain the exosome. The collected pellet was mixed with 1.5 times PBS buffer and filtered through a 0.8-μm filter, and then, the Exosupur Reagent (Echobiotech, Beijing, China) was used to isolate and purify the exosomes according to the manufacturer's instructions. The pellet was resuspended in 0.01 M PBS buffer and concentrated in an Amicon Ultra-4 centrifuge filter device with 100 kDa exclusion (MilliporeSigma, Burlington, MA, USA) at 200 μl, and exosomes were obtained.

Characterization of isolated exosomes

For transmission electron microscopy (TEM) of exosomes, a 10 μl sample was dropped onto a Formvar carbon-coated electron microscope grid (Leica Microsystems, Buffalo Grove, IL, USA). After 10 min of absorbing, the grid was washed with distilled water and blotted with filter paper, then touched with a solution of 2% uranyl acetate for 1 min on the surface of the grid, removing excess uranyl acetate and drying the surface of the grid under an incandescent lamp for 2 min. The size and morphology of the exosomes were observed using the H-7650 transmission electron microscope (Hitachi Ltd., Tokyo, Japan).

Determination of the average size and particle concentration of exosomes was done by nanoparticle tracking analysis (NTA) using the ZetaView PMX 110 (Particle Metrix, Meerbusch, Germany). A 60 s video is captured at 30 frames/s under a wavelength of 405 nm. The data were analyzed using the ZetaView v.8.02.28 NTA software.

The exosomal surface protein markers were identified by Western blotting. The exosomes proteins concentration was quantified using the BCA Protein Assay Kit (Beyotime, Beijing, China). Cell lysate of A549 cells (human non-small cell lung cancer cells) was used as control. Equal amounts (50 μg) of protein were resolved by SDS-PAGE using a 10% polyacrylamide gel and transferred to PVDF membranes. The membranes were blocked with 5% non-fat milk in Tris-buffered saline containing 0.1% Tween-20 (TBS-T) for 1 h at room temperature and then incubated overnight at 4 °C with the anti-CD63 antibody (Santa Cruz, CA, USA), anti-CD9 antibody (Proteintech, Rosemont, IL), anti-Tsg101 antibody (Santa Cruz, CA, USA) and anti-Calnexin antibody (Promega, Madison, WI). All antibodies were used at a 1:1000 dilution. The membranes were washed three times with TBS-T and incubated with horseradish peroxidase-conjugated anti-mouse or anti-rabbit secondary antibody (Santa Cruz, CA, USA) for 1 h at room temperature and rewashed three times with TBS-T. Immunoreactive bands were visualized with an ECL detection kit (MilliporeSigma) and scanned in the Tanon 4600 automatic chemiluminescence image system (Tanon, Shanghai, China).

Table 1 Preoperative characteristics and clinical data of patients in the RNA sequencing step

Parameter	POAF patients ($n=6$)	non-POAF patients ($n=6$)	P value
Age (years)	62.17 ± 3.77	64.50 ± 5.28	0.653
Gender (%male)	83.33	66.67	0.234
BMI (kg/m^2)	27.84 ± 3.95	26.77 ± 2.94	0.354
Hypertension	4	4	1
Diabetes	2	5	0.234
Hypercholesterolemia	4	6	1
Smoking	2	3	0.448
Drinking	3	1	0.073
Stroke	0	1	0.031
Chronic lung disease	0	0	1
PMI	0	1	0.031
PCI	1	0	0.031
CRP	2.68 ± 2.23	6.98 ± 7.58	0.125
WBC	8.02 ± 2.17	8.75 ± 1.77	0.569
PLT	222.17 ± 49.56	251.83 ± 32.49	0.570
ALT	36.50 ± 29.41	33.00 ± 20.55	0.588
CREA	86.78 ± 17.96	69.82 ± 13.67	0.490
UA	349.98 ± 66.92	291.58 ± 70.43	0.767
TG	1.20 ± 0.12	1.37 ± 0.45	0.09
LDL	2.69 ± 1.63	2.54 ± 0.43	0.058
HDL	1.14 ± 0.20	1.09 ± 0.18	0.643
hypokalemia	2	3	0.599
hypoxia	0	3	1.000
hypovolemia	2	2	0.049
hypoglycemia	0	1	0.341
pain	3	1	0.260
anemia	2	4	0.290
EF	62.67 ± 7.26	60.00 ± 7.40	1
LAD	37.17 ± 4.53	36.17 ± 2.71	0.653
LVEDD	51.17 ± 6.70	44.67 ± 3.27	0.013
LVSDD	33.17 ± 5.84	29.00 ± 1.89	0.045
IABP	2	0	0.001
In-hospital days	21.67 ± 4.88	14.83 ± 3.12	0.016
LIMA used	5	3	0.073
Grafts	4.17 ± 0.41	4.50 ± 0.55	0.943

BMI, body mass index; PMI, preoperative myocardial infarction; PCI, percutaneous coronary intervention; CRP, C-reactive protein; WBC, white blood cell; PLT, platelet; ALT, alanine aminotransferase; CREA, creatinine; UA, uric acid; TG, triglyceride; LDL, low-density lipoprotein; HDL, high-density lipoprotein; EF, ejection fraction; LAD, left atrial diameter; LVEDD, left ventricular end-diastolic dimension; LVSDD, left ventricular end-systolic dimension; IABP, intra-aortic balloon pump; LIMA, left internal mammary artery

Exosomal RNA extraction and miRNA sequencing

Total RNA was extracted from isolated exosomes using the miRNeasy Mini Kit (Qiagen, Hilden, Germany), and the RNA concentration was measured using the RNA Nano 6000 Assay Kit (Qiagen) and Agilent Bioanalyzer 2100 System (Agilent Technologies, CA, USA). The RNA sample (1 ng-500 ng) was processed with adapter ligation, cDNA synthesis, PCR amplification, and the construction of RNA libraries with the QIAseq miRNA library kit (Qiagen, Frederick, MD). Then, RNA sequencing was performed on the Illumina-HiSeq2500 sequencing platform (Illumina, CA, USA). Finally, more than 20 million reads sequencing depth of datasets were generated, and the raw data were filtered to obtain high-quality reads and then compared with the Silva, GtRNAdb, Rfam and Repbase databases, and filtered out the rRNA, tRNA, snRNA, snoRNA, other ncRNAs, and repeat sequences. The unannotated reads were matched with the

Table 2 Preoperative characteristics and clinical data of patients in the validation step

Parameter	POAF patients ($n=10$)	non-POAF patients ($n=10$)	P value
Age (years)	61.80 ± 5.79	65.30 ± 4.29	0.142
Gender (%male)	90.00	80.00	0.556
BMI (kg/m^2)	25.31 ± 3.69	24.37 ± 2.39	0.506
Hypertension	7	6	0.660
Diabetes	2	5	0.660
Hypercholesterolemia	4	6	0.074
Smoking	2	3	0.673
Drinking	3	1	1
Stroke	0	1	0.331
Chronic lung disease	0	0	1
PMI	0	1	0.556
PCI	1	1	1
CRP	3.60 ± 3.84	1.26 ± 1.18	0.093
WBC	7.00 ± 1.97	7.24 ± 1.32	0.747
PLT	205.70 ± 41.97	224.70 ± 39.57	0.311
ALT	26.90 ± 11.68	28.40 ± 22.59	0.854
CREA	77.40 ± 11.96	78.62 ± 10.23	0.810
UA	344.97 ± 64.67	340.98 ± 75.89	0.901
TG	2.56 ± 1.82	1.42 ± 0.61	0.088
LDL	2.51 ± 1.02	2.77 ± 1.41	0.644
HDL	1.05 ± 0.22	1.04 ± 0.23	0.977
hypokalemia	3	1	0.290
hypoxia	1	1	1.000
hypovolemia	6	1	0.020
hypoglycemia	0	0	1
pain	4	4	1
anemia	0	3	0.081
EF	59.50 ± 10.17	63.90 ± 5.42	0.243
LAD	38.90 ± 6.45	35.50 ± 2.99	0.155
LVEDD	53.10 ± 6.23	45.90 ± 4.82	0.010
LVSDD	37.80 ± 8.23	30.60 ± 6.27	0.041
IABP	2	0	0.168
In-hospital days	28.30 ± 17.20	15.40 ± 4.55	0.044
LIMA used	8	8	1
Grafts	4.30 ± 0.67	4.30 ± 0.67	1

BMI, body mass index; PMI, preoperative myocardial infarction; PCI, percutaneous coronary intervention; CRP, C-reactive protein; WBC, white blood cell; PLT, platelet; ALT, alanine aminotransferase; CREA, creatinine; UA, uric acid; TG, triglyceride; LDL, low-density lipoprotein; HDL, high-density lipoprotein; EF, ejection fraction; LAD, left atrial diameter; LVEDD, left ventricular end-diastolic dimension; LVSDD, left ventricular end-systolic dimension; IABP, intra-aortic balloon pump; LIMA, left internal mammary artery

miRBase database and Human Genome (GRCh38) to reveal known miRNAs. Exosomal miRNAs data obtained from the POAF and non-POAF groups were compared, and the edgeR algorithm is used to analyze differential expression of miRNAs (DEMs), Transcripts per million (TPM) > 10, $|\log_2 FC| > 0.584$ and $p < 0.05$ were taken as DEMs identification thresholds. A heat map for cluster analysis was created based on normalized log(TPM + 1) values featuring miRNAs with remarkable differences.

Prediction and gene function enrichment analysis of miRNA target genes

The potential target genes for DEMs were predicted by the R script using the multiMiR package. Gene Ontology (GO) (http://geneontology.org/) and Kyoto Encyclopedia of Genes and Genomes (KEGG) pathway enrichment analysis (http://www.genome.jp/kegg/) were performed to identify biological processes (BP), molecular function (MF), cellular components (CC) and KEGG pathways of the predicted target genes involved. The *p*-value was calculated by hypergeometric distribution, and then, the *q*-value was acquired by BH correction.

Real-time PCR validation

Reverse transcription of total exosomal RNA to cDNA using the PrimeScript™ RT reagent kit (RR037A, TAKARA, Tokyo, Japan) and then measured by TaKaRa Ex Taq Hot Start Version (RR006A, TAKARA) with predesigned probes. The miRNA expression levels were analyzed by LC480 and calculated using the $2^{-\Delta\Delta Ct}$ method, with U6 acting as the internal reference. The sequences of the primers and probes are shown in Table 3.

Luciferase reporter assay

Wild-type (WT) and mutated 3'-UTR fragments of PDK4 position 1010–1017 (MUT) pMIR-REPORT luciferase vectors and mimic miR-122-5p were purchased from Echo Biotech (Beijing, China). HEK293T cells were purchased from ATCC and incubated in DMEM medium (Sigma, St. Louis, MI, USA) with 10% FBS, cultured in a humidified incubator with 5% CO_2 at 37 °C. The REPORT WT/MUT vectors and miR-122-5p mimics were cotransfected into HEK293T cells, and the activity of luciferase was detected by Luciferase reporter assays (Promega, Madison, WI, USA) according to the manufacturer's instructions. Normalized luciferase activity was assayed in HEK293T cells lysates 24 h after transfection.

Statistical analysis

Statistical analysis was performed using the GraphPad Prism software version 9.0 (GraphPad Software, La Jolla, CA, USA). Comparisons between the two groups were analyzed

Table 3 The primer sequences for real-time PCR

Common reverse primer	GTGCAGGGTCCGAGGT
cel-miR-39-RT	GTCGTATCCAGTGCAGGGTCCGAGGTATTCGCACTGGATACGACCAAGCT
cel-miR-39-F	CGCTCACCGGGTGTAAATC
cel-miR-39-P	ATTCGCACTGGATACGACCAAGCT
U6-RT	AACGCTTCACGAATTTGCGT
U6-F	CTCGCTTCGGCAGCACA
U6-R	AACGCTTCACGAATTTGCGT
U6-P	AGAAGATTAGCATGGCCCCTGCGCA
hsa-miR-26b-5p-RT	GTCGTATCCAGTGCAGGGTCCGAGGTATTCGCACTGGATACGACACCTAT
hsa-miR-26b-5p-F	CCGACCTGTTCAAGTAATTCAG
hsa-miR-26b-5p-P	TTCGCACTGGATACGACACCTATC
hsa-miR-122-5p-RT	GTCGTATCCAGTGCAGGGTCCGAGGTATTCGCACTGGATACGACCAAACAC
hsa-miR-122-5p-F	CCGCTGGAGTGTGACAATG
hsa-miR-122-5p-P	TCGCACTGGATACGACCAAACAC
hsa-miR-191-5p -RT	GTCGTATCCAGTGCAGGGTCCGAGGTATTCGCACTGGATACGACCAGCTG
hsa-miR-191-5p -F	AGCCAACGGAATCCCAAAAG
hsa-miR-191-5p -P	TCGCACTGGATACGACCAGCT
hsa-miR-181a-5p-RT	GTCGTATCCAGTGCAGGGTCCGAGGTATTCGCACTGGATACGACACTCAC
hsa-miR-181a-5p-F	GCAACATTCAACGCTGACG
hsa-miR-181a-5p-P	TTCGCACTGGATACGACACTCAC
hsa-miR-155-5p -RT	GTCGTATCCAGTGCAGGGTCCGAGGTATTCGCACTGGATACGACAACCCC
hsa-miR-155-5p -F	ACGGCTATTAATGCTAATCGTGATA
hsa-miR-155-5p -P	TTCGCACTGGATACGACAACCCC
hsa-miR-151a-5p -RT	GTCGTATCCAGTGCAGGGTCCGAGGTATTCGCACTGGATACGACACTAGA
hsa-miR-151a-5p -F	CGGTCGAGGAGCTCACA
hsa-miR-151a-5p -P	TTCGCACTGGATACGACACTAGAC

F, forward primer; R, reverse primer; RT, reverse transcription; P, probe

using two-tailed unpaired Student's t-tests. Categorical data were compared using the Chi-square test or Fisher's exact method. Values of $p < 0.05$ were considered significant. The receiver operating characteristic (ROC) curve was established to evaluate the diagnostic value. The cut-off value of miRNA was analyzed by SPSS 22 software (IBM, Armonk, NY, USA).

Results

Clinical characteristics of patients

The demographic and clinical baseline characteristics of the participants enrolled in our study are shown in Table 1 and Table 2. Among these parameters, the left ventricular end-diastolic dimension (LVEDD) and the left ventricular end-systolic dimension (LVSDD) were significantly different between the POAF and non-POAF groups ($p < 0.05$), which indicated that changes in cardiac structure and heart function may be related to POAF progression. However, there were no significant differences in left atrial diameter (LAD) between the POAF and non-POAF groups ($p > 0.05$), indicating that there were no significant changes in the left atrium in the POAF group. In-hospital days were significantly different between the POAF and non-POAF groups ($p < 0.05$), and POAF patients stayed longer than non-POAF patients. Furthermore, among the important risk factors for POAF, such as hypokalemia, hypoxia, hypoglycemia, hypovolemia, pain and anemia, hypovolemia was significantly different between the POAF and non-POAF groups ($p < 0.05$), which indicated that hypovolemia can increase the risk of POAF.

Characterization of plasma exosomes

Characterization of isolated plasma exosomes was identified by TEM, NTA, and Western blot analysis. TEM revealed that the exosome-shaped particle structures, oval or bowl-shaped capsules, had no nucleus (Fig. 1A), which size and morphology were consistent with the exosome characteristics. NTA analysis revealed that the mean size of the exosomes was about 30–150 nm in diameter, which are considered exosomes (Fig. 1B). The exosomal surface protein

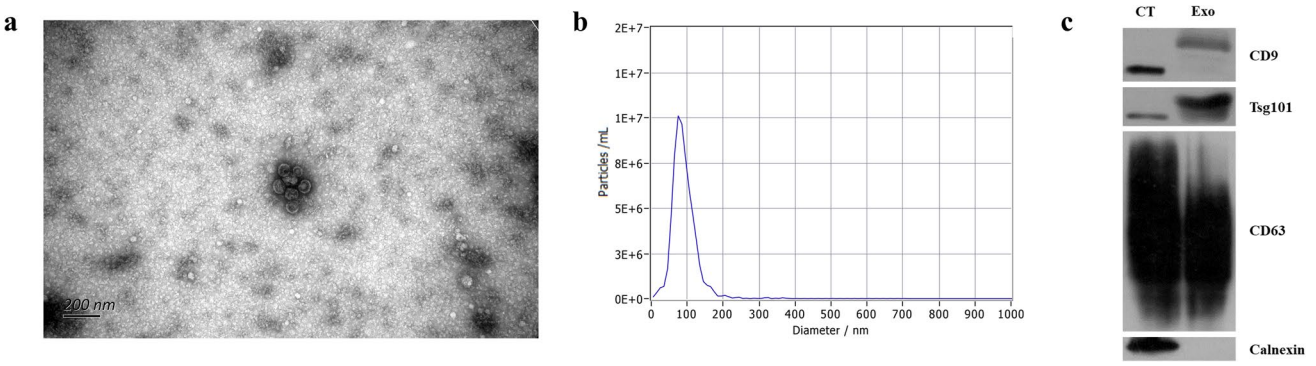

Fig. 1 Characterization of plasma exosomes. (**a**) TEM images showed that exosomes were oval or bowl-shaped capsules and had no nucleus (scale bar = 200 nm). (**b**) NTA analysis showed that the mean size of the exosomes was about 30–150 nm in diameter. (**c**) Western blot analysis demonstrated the expression of exosomal marker proteins, CD9, CD63, Tsg101, and negative marker proteins Calnexin in isolated exosomes. CT, control; Exo, exosomes

markers CD9, CD63, and Tsg101, as well as the negative marker Calnexin, were identified by Western blotting. As shown in Fig. 1C, the CD9, CD63, and Tsg101 protein bands were visible in isolated plasma exosomes, and no expression of Calnexin was found, indicating the purity of the isolated plasma exosomes.

Identification of exosomal differentially expressed miRNAs

The miRNA sequencing was performed to identify exosomal differentially expressed miRNAs (DEMs) between the POAF ($n = 6$) and non-POAF ($n = 6$) groups, TPM > 10, $|\log_2 FC| > 0.584$ and $p < 0.05$ were used as the identification threshold for DEMs. Principal component analysis (PCA) showed that the individuals of POAF and non-POAF groups were significantly different (Fig. 2A), and the hierarchical clustering heatmap showed differentially expressed miRNAs (Fig. 2B). Finally, a total of 23 exosomal miRNAs were found to be differentially expressed between the POAF and non-POAF groups, among which 17 miRNAs were up-regulated and 6 miRNAs were down-regulated (Table 4). Furthermore, the specificity and sensitivity of each DEM were calculated (Fig. 2C). As shown in Table 4, most DEMs showed a sensitivity of 0.8–1.0 and a specificity of 0.6–1.0.

Gene ontology (GO) enrichment and KEGG annotation analysis

To understand the comprehensive function of exosomal miRNAs, DEMs target genes were predicted using the multiMiR package, followed by GO and KEGG analysis through the GO and KEGG databases. Three types of functional annotations were performed: biologic process, cell composition, and molecular function. A variety of GO enrichment and KEGG annotation terms were enriched, and the top 20 GO and KEGG terms are shown in Fig. 3. The biological processes such as the Positive regulation of NF-kappa B transcription factor activity and the Negative regulation of apoptotic process (Fig. 3A), cellular components such as the Extracellular exosome and the Endosome membrane (Fig. 3B), and molecular functions such as the zinc ion binding and the Metal ion binding (Fig. 3C), and KEGG pathways, such as the TNF signaling pathway and the MAPK signaling pathway, were enriched, which may be related to the biological process of POAF. The results of the functional analysis above provide a possible theoretical basis for the development of POAF.

qRT-PCR verification of exosomal differentially expressed miRNAs

Based on function analysis and the most significant fold changes of the DEMs, miR-122-5p, miR-191-5p, miR-181a-5p, miR-155-5p, and miR-151a-5p were selected for qRT-PCR validation. As shown in Fig. 4A, miR-122-5p was up-regulated in POAF patients (AF group) compared to non-POAF patients (CT group), but there are no significant changes in miR-191-5p, miR-181a-5p, miR-155-5p and miR-151a-5p (Fig. 4B-4E). To evaluate the potential diagnostic value of miR-122-5p, a ROC curve was generated for miR-122-5p levels in plasma samples from POAF patients. As shown in Fig. 4F, the area under the ROC curve (AUC) was 0.79 ($p = 0.028$), and the 95% confidence interval is 0.58 to 1.00.

Functional analysis and determination of the miR-122-5p target genes

To gain further insight into the functions of miR-122-5p and its target genes, GO enrichment and KEGG annotation analysis were performed focused on heart functions. The

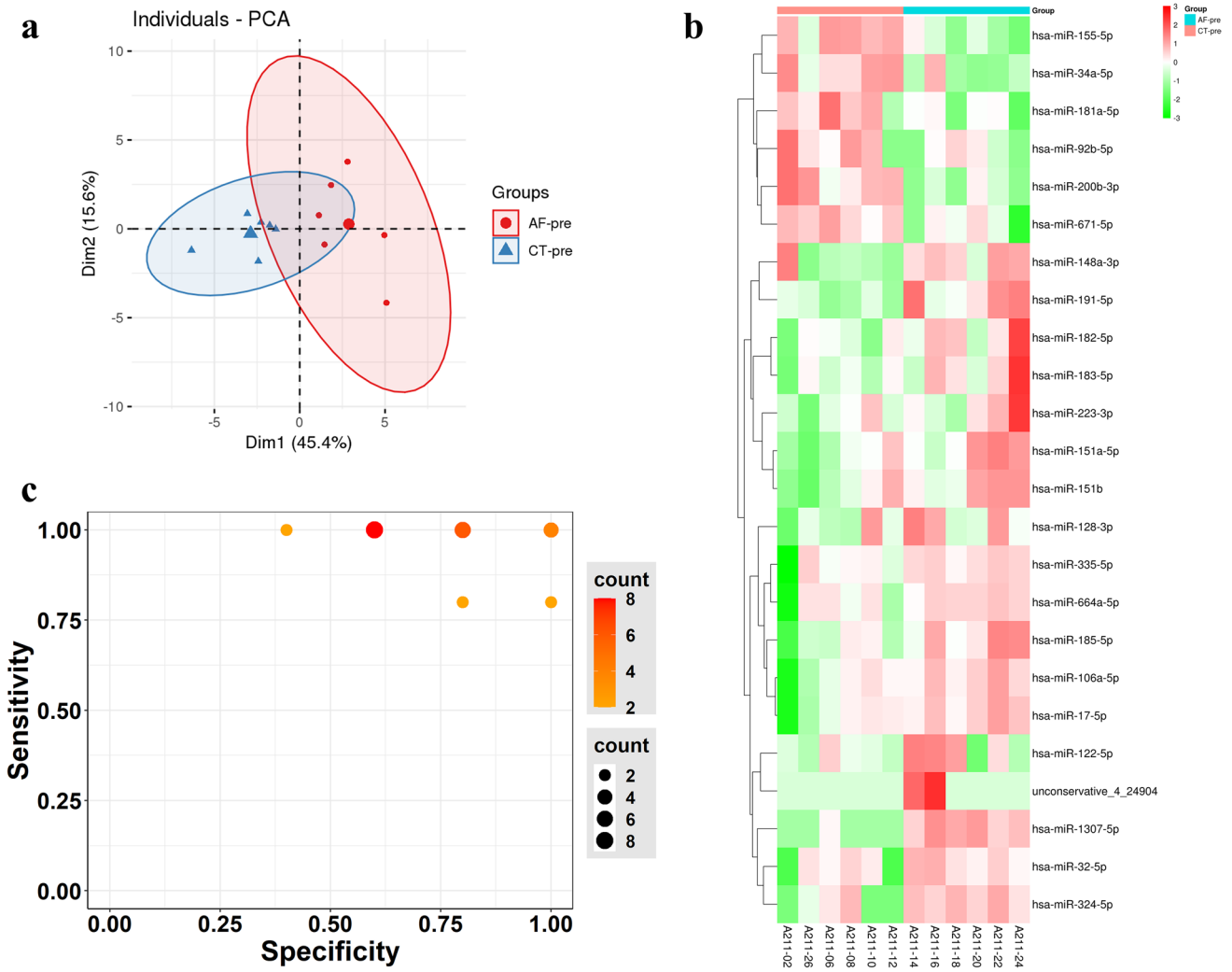

Fig. 2 Identification of exosomal differentially expressed miRNAs (DEMs). (**a**) PCA analysis of the POAF group (AF-pre) and non-POAF group (CT-pre) of patients. (**b**) The specificity and sensitivity of each DEM in identifying exosomes from POAF patients. (**c**) Heat-map of DEMs in the POAF group (AF-pre) and non-POAF group (CT-pre) of the patients. The intensity plot shows the relatively higher expression (red) and the lower expression (green)

circos diagram of the KEGG annotation showed that inflammation-related pathways, such as the NF-kappa B signaling pathway (NFKB1A, IL1R1, ERC1 and TNFSF11), the Toll-like receptor signaling pathway (MAPK1, IL6, AKT1, CXCL9), and the TGF-beta signaling pathway (MAPK1, TGFB1, TGFBR1 and MYC), were enriched, and the target genes were separated on different chromosomes. GO enrichment networks were shown that the regulation of cardiac muscle contraction by regulation of the release of sequestered calcium ion (TNNC2, CALM2, CLIC1 and CLIC4), the Negative regulation of toll-like receptor signaling pathway (PDK4, IRAK3, PDPK1 and IRF9), and the Regulation of oxidative stress-induced intrinsic apoptotic signaling pathway (AKT1, MAPK1, NFE2L1 and NFE2L3), were closely related to cardiac functions to promote apoptosis, fibrosis, and hypertrophy, and play a promoting role in cardiac fibrosis (Fig. 5B). Furthermore, the Luciferase reporter assay verified that miR-122-5p directly regulates the PDK4 gene (Fig. 6), which is involved in the Negative regulation of toll-like receptor signaling pathway.

Discussion

POAF occurs primarily in the postoperative period after cardiac surgery [20]. Although many interventions have been proposed to prevent the occurrence of POAF, prevention protocols have not been routinely implemented [21]. Starting before or during cardiac surgery is the most effective way to prevent POAF, so it is very important to identify intermediate-risk and high-risk patients prior to surgery [22], and miRNAs in plasma exosomes are convenient and

Table 4 Differentially expressed miRNAs in isolated exosomes of POAF patients

miRNA ID	P-value	log_2FC	Sensitivity	Specificity	AUC
hsa-miR-106a-5p	0.019812	0.817176	1	0.6	0.88
hsa-miR-122-5p	0.014876	1.322265	1	0.6	0.8
hsa-miR-128-3p	0.047438	0.783448	0.8	0.8	0.84
hsa-miR-1307-5p	5.79E-05	2.993741	1	1	1
hsa-miR-148a-3p	0.017885	0.762074	0.8	1	0.8
hsa-miR-151a-5p	0.018992	0.81471	1	0.6	0.88
hsa-miR-151b	0.030293	0.843204	1	0.6	0.88
hsa-miR-155-5p	0.001215	-0.85977	1	0.8	0.96
hsa-miR-17-5p	0.013669	0.886672	1	0.6	0.88
hsa-miR-181a-5p	0.019374	-0.90891	1	1	1
hsa-miR-182-5p	0.012417	1.002605	1	0.8	0.92
hsa-miR-183-5p	0.002493	1.523433	1	0.8	0.88
hsa-miR-185-5p	0.00168	1.104072	1	0.6	0.84
hsa-miR-191-5p	0.000189	0.911508	1	1	1
hsa-miR-200b-3p	7.72E-05	-3.65012	1	1	1
hsa-miR-223-3p	0.04233	0.71342	1	0.4	0.68
hsa-miR-32-5p	0.041102	1.116165	1	0.6	0.84
hsa-miR-324-5p	0.02	1.523033	0.8	1	0.88
hsa-miR-335-5p	0.027803	0.976818	0.8	0.8	0.8
hsa-miR-34a-5p	0.009433	-1.32052	1	0.8	0.88
hsa-miR-664a-5p	0.044844	0.944237	1	0.8	0.88
hsa-miR-671-5p	0.015001	-1.57193	1	0.8	0.96
hsa-miR-92b-5p	0.026431	-2.13423	1	0.6	0.88

effective potential biomarkers for the diagnosis of POAF. Approximately 10–15% of circulation miRNAs are composed of exosomal miRNAs, and exosomes deliver the specific miRNA and then regulate gene expression in recipient cells [23]. Since miRNAs are more stable in exosomes than in other blood components, measuring miRNA in exosomes has higher sensitivity and specificity than in total biological fluids [24]. Although many studies have shown a close relationship between exosomes and cardiovascular disease, the correlation between exosomes and POAF remains unclear.

Our study is the first transcriptomic study to explore and analyze the pathogenesis of POAF using high-throughput RNA sequencing and identifying the exosomal different expression miRNAs (DEMs). Using high-throughput RNA sequencing, we revealed 23 miRNAs that were significantly different expressions between the POAF and non-POAF groups. Furthermore, the GO and KEGG enrichment analyses of DEMs target genes revealed that these miRNAs can affect atrial structure through many signaling pathways in POAF pathogenesis.

The clinical characteristics of patients showed that the LVEDD and LVSDD were significantly decreased in POAF groups but no changes in LAD, and the POAF risk factors hypovolemia was significantly different between the POAF and non-POAF groups, indicating that changes in cardiac structure and heart function can increase the risk of POAF. In addition, the POAF patients' in-hospital days were longer than non-POAF patients. In our study, the non-POAF patients were asked to receive ECG examinations 3 months after discharge. No atrial fibrillation or any arrhythmia cases were observed during their follow-up. However, we regretted that no patients experienced Holter postoperatively, so we could not get more precise results in terms of patients' cardiac rhythm, which is one of this study's limitations. In our future study, more measures such as Holger and remote sensing equipment will be taken so that we can monitor the cardiac rhythms of patients after cardiac surgeries more accurately. Furthermore, when patients in the POAF group had atrial fibrillation during hospitalization, patients in the non-POAF group had not been discharged, which indicated that the time of atrial fibrillation in the POAF group was shorter than that in-hospital day of the non-POAF group.

Based on analysis of atrial fibrillation-related gene function and the most significant fold changes of each DEMs, miR-122-5p, miR-191-5p, miR-181a-5p, miR-155-5p, and miR-151a-5p were selected for qRT-PCR validation. We found that miR-122-5p was up-regulated in the POAF patients, but there have been no significant changes in miR-191-5p, miR-181a-5p, miR-155-5p, and miR-151a-5p. The ROC curve showed that the miR-122-5p has high sensitivity and specificity in the diagnosis of POAF. Furthermore, miR-122-5p target genes were involved in many pathways related to heart functions, such as the NF-kappa B signaling pathway, the Negative regulation of toll-like receptor signaling pathway, and the Regulation of oxidative stress-induced intrinsic apoptotic signaling pathway. Our findings indicated that plasma exosomal miRNAs can be used as novel biomarkers to diagnose POAF.

MiR-122 has various effects on the cardiovascular system by regulating cardiovascular inflammation, autophagy,

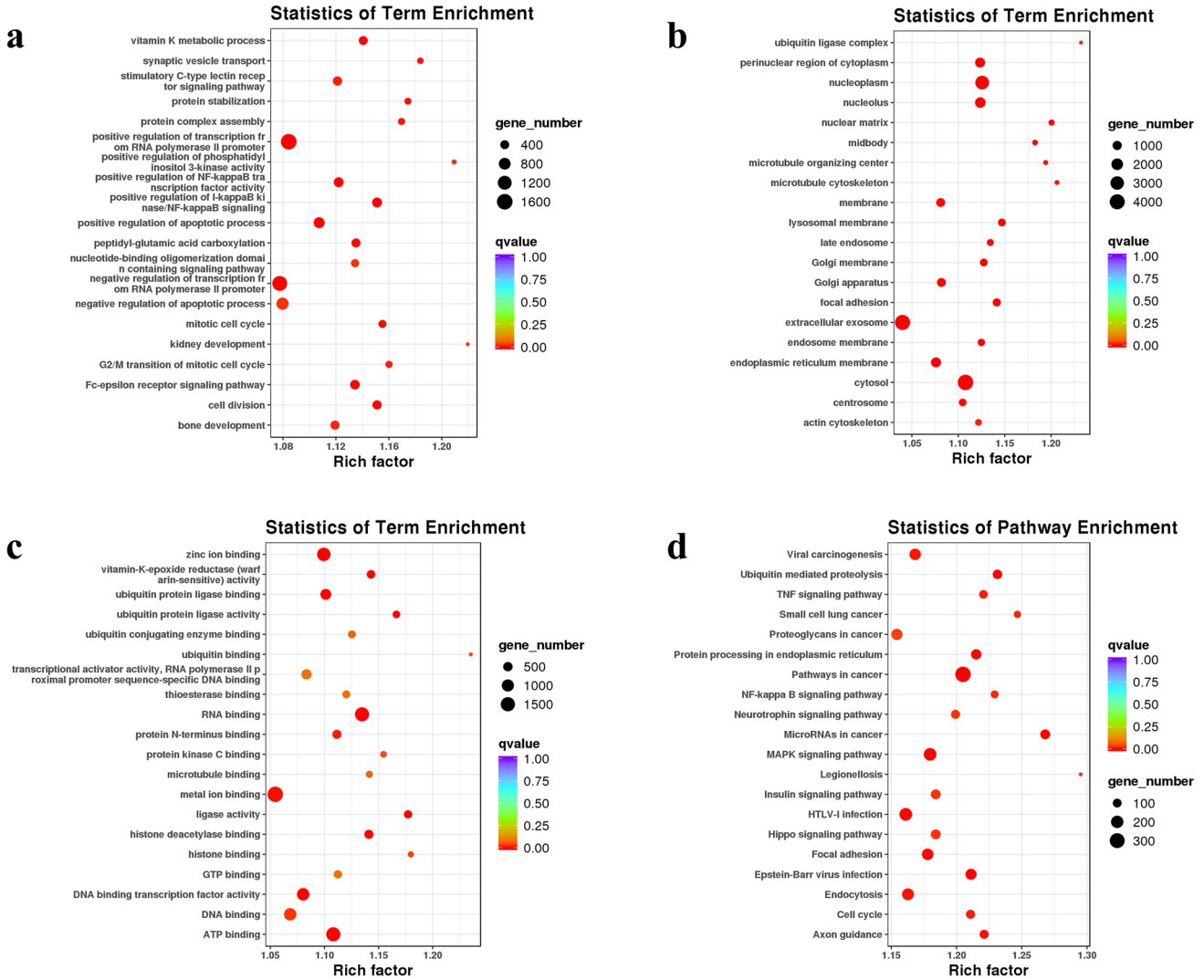

Fig. 3 Gene ontology (GO) enrichment and KEGG annotation analysis of DEMs' target genes. (**a**) The bubble plot of enriched biological processes. (**b**) The bubble plot of enriched cellular components. (**c**) The bubble plot of enriched molecular functions. (**d**) The bubble plot of KEGG annotation. The number of genes enriched in each term is shown as the circle size, and the p-value is shown as different colors

apoptosis, oxidative stress, fibrosis, and dysfunction through its target genes, which is a promising biomarker for the diagnosis of cardiovascular diseases [25–27]. Previous studies have shown that miR-122 can predict the risk of AF [28, 29]. On the one hand, miR-122 levels increased significantly in the AF mice model [30]; On the other hand, the high expression of miR-122 involved in the proliferation and apoptosis of CMs by regulating the expression of anti-apoptotic proteins, such as Bcl-2 and caspase-3, in atrial fibrillation [28], indicating that increased miR-122 may predict and involve POAF development. We found that miR-122-5p was up-regulated in plasma exosomes of POAF patients, indicating that interference expression of miR-122-5p may be a strategy for the prevention and treatment of POAF. However, miR-122-5p was not well known in the study of POAF, which may be of interest for future research.

The gene enrichment analysis of the miR-122-5p target genes showed that the Toll-like receptor signaling pathway is closely related to the progression of POAF. Innate immune factors play an important role in most cardiac diseases [31, 32], especially Toll-like receptors (TLRs), and TLRs can participate in the pathophysiological progression of coronary disease [33]. The previous study has shown that TLR2, TLR4, and their downstream signal proteins were significantly increased in patients with new-onset atrial fibrillation after acute myocardial infarction, which has the potential to diagnose the disease [34]. Another study showed that peripheral monocyte Toll-like receptor (TLR) expression was associated with AF presence, indicating that

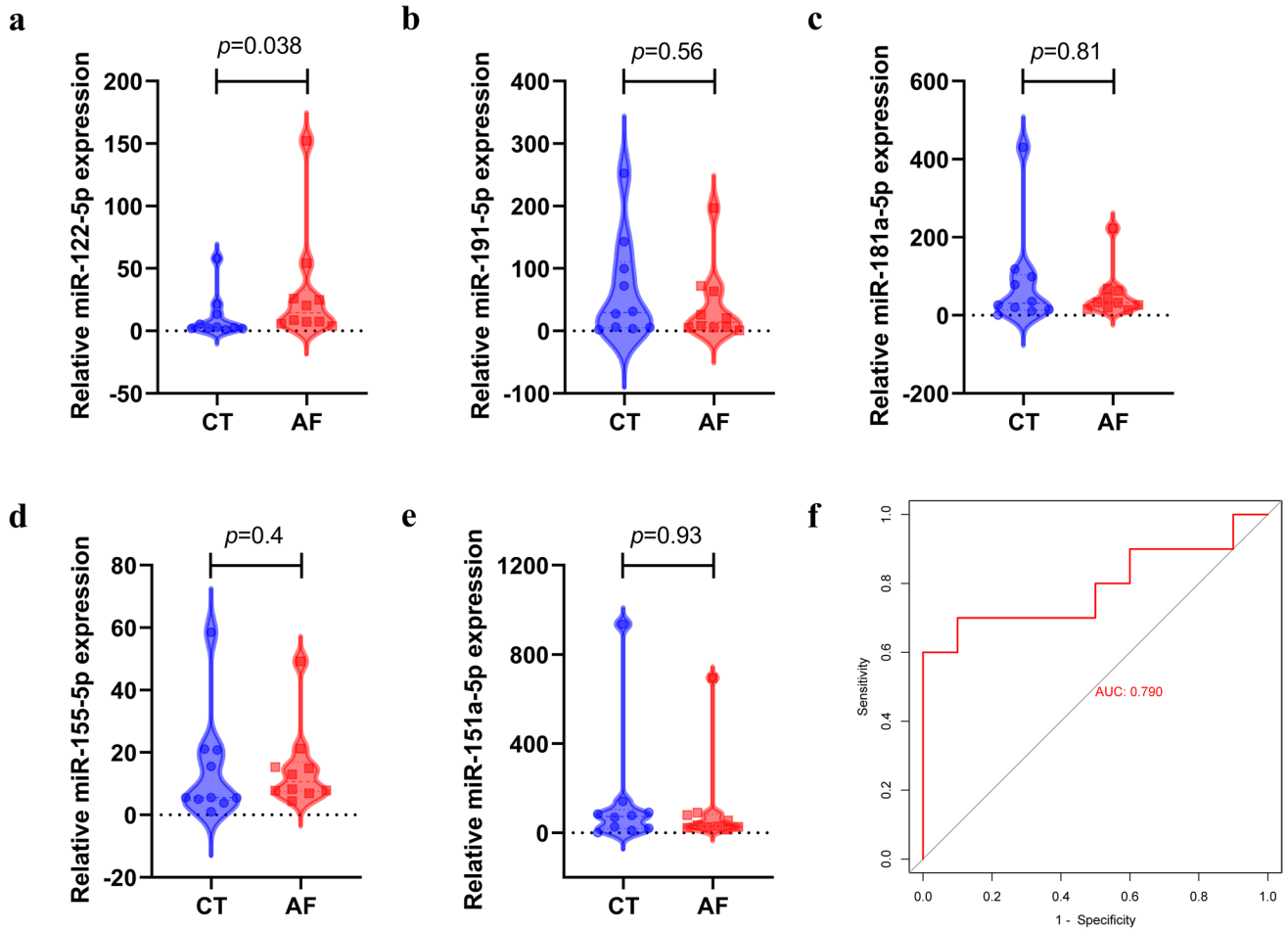

Fig. 4 qRT-PCR quantitation of exosomal differentially expressed miRNAs expressions levels. The expression levels of miR-122-5p (**a**), miR-191-5p (**b**), miR-181a-5p (**c**), miR-155-5p (**d**) and miR-151a-5p (**e**) in plasma samples of the control (CT) and AF groups ($n = 10$ in each group). (**f**) Receiver operating characteristic (ROC) curve of miR-122-5p levels in plasma samples from POAF patients

TLR-mediated inflammation plays an important role in the pathogenesis of AF [35].

Among the miR-122-5p target genes, we demonstrated the regulation of miR-122-5p in the pyruvate dehydrogenase kinase 4 (PDK4) by the luciferase reporter assay, which participates in the Negative regulation of toll-like receptor signaling pathway. PDK4 regulates the pyruvate dehydrogenase complex (PDC) [36], which plays a key role in glucose metabolism. Elevated expression of PDK4 inactivates PDC and promotes gluconeogenesis [37]. Recent studies have demonstrated the importance of energy metabolism in the development of AF [38, 39], and changes in PDK4 may response to cardiometabolic demands and correlate with AF burden [40]. However, the relationship between miR-122-5p and PDK4 in the progression of POAF is unclear, which needs to be explored in future studies.

Abnormal expression of miR-191 has been reported in various diseases, such as cancer, pulmonary hypertension, type 2 diabetes, and Alzheimer's disease [41]. A recent study has shown that miR-191 is one of the most represented miRNAs in ASCs-derived exosomes (ASCs-Exos) [42], and is also elevated in the circulation of patients with pulmonary arterial hypertension (PAH) [43]. The miR-181a-5p has been shown to participate in hypoxia–reoxygenation-induced cardiomyocytes apoptosis by regulating SIRT1, which could become a novel direction for related diseases [44]. The miR-155-5p was up-regulated in plasma exosome and valve tissues from the rat model with rheumatic heart disease and regulated the progression of valvular damage by regulating multiple signaling pathways [45]. The previous study also showed that miR-151a-5p and miR-181a-5p were significantly correlated with cardiovascular risk factors in coronary artery disease [46]. However, miR-191-5p, miR-181a-5p, miR-155-5p, and miR-151a-5p were not well known in the study of cardiac diseases. In this regard, the PCR results revealed a significant increase in miR-122-5p in plasma from POAF patients, indicating a potential role of miR-122-5p in the pathogenesis of POAF.

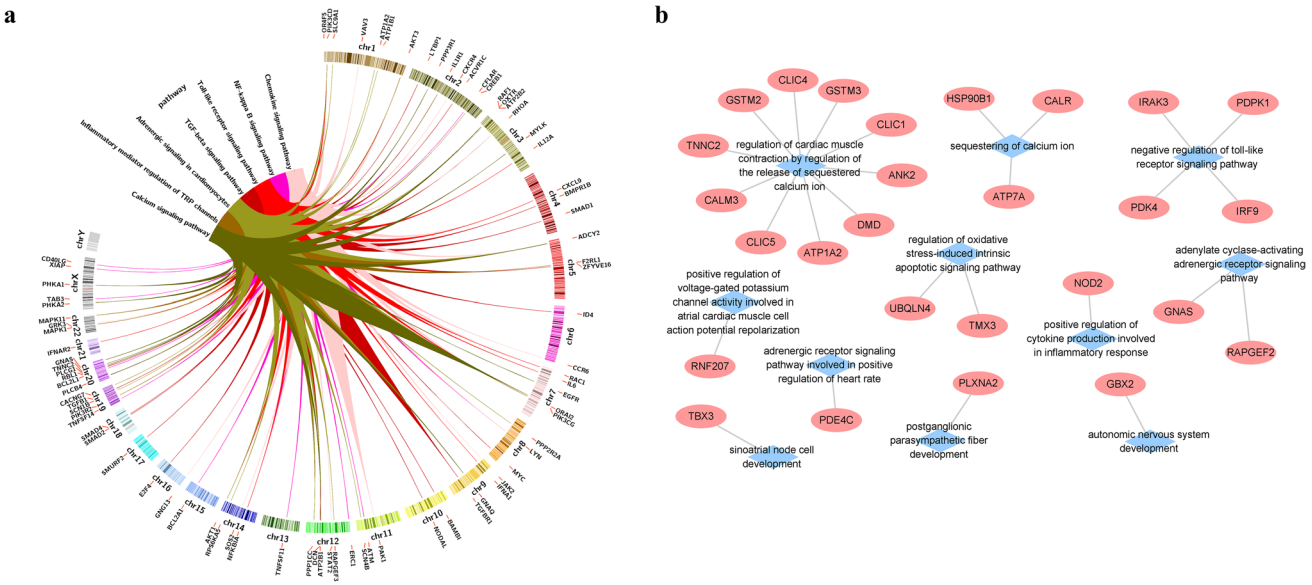

Fig. 5 GO enrichment and KEGG annotation analysis of miR-122-5p target genes. (**a**) Circos diagram of KEGG annotation analysis of miR-122-5p target genes. Each color represents one KEGG term and the gene locations on each chromosome. (**b**) GO enrichment network of miR-122-5p target genes

In conclusion, we found 23 differentially expressed exosomal miRNAs and validated 5 of them (miR-122-5p, miR-191-5p, miR-181a-5p, miR-155-5p and miR-151a-5p) by qRT-PCR. The miR-122-5p may be related to many signaling pathways that can affect atrial function and structure, oxidative stress, and fibrosis involved in the progression of POAF. Our findings provided new perspectives on the mechanisms of exosome miRNA and POAF. Exosomal miRNAs have great potential as novel biomarkers to assess the severity or prognostic of POAF, which may contribute to risk stratification, individualized therapeutic strategy, drug intervention, and evaluation of POAF. Although exosomes show attractive possibilities in the diagnosis and treatment of cardiovascular diseases, these new methods are still undeveloped areas that we are committed to developing.

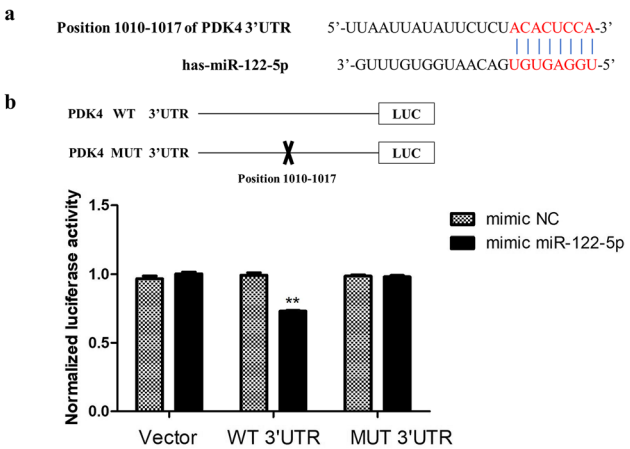

Fig. 6 MiR-122-5p directly regulates PDK4. (**a**) The predicted binding sequences between miR-122-5p and target sites in PDK4 3'-UTR. (**b**) The pMIR-REPORT luciferase vectors of the wild-type (WT) or mutated 3'UTR fragments of PDK4 position 1010–1017 (MUT) was co-transfected with miR-122-5p mimics into HEK293T cells, and the luciferase activity was evaluated by luciferase reporter assays. Normalized luciferase activity in HEK293T cells lysates was assayed 24 h after transfection. Data represent as Mean ± SD, n = 3, $^{**}p < 0.01$ versus mimic normal control (NC)

Acknowledgements This study was supported by the National Natural Science Foundation of China (No. 81770320, 82170311) to J. Wang.

Author Contributions C.B. and Y.L. contributed to writing—original draft preparation. C.B., Y.Z., Q.Y. and C.Z. contributed to software, data curation. C.B. and Y.L. contributed to resources, validation. J.W. contributed to writing—reviewing and editing, supervision. All authors approved the manuscript for publication.

Declarations

Ethics Statement All procedures performed in the study have been approved by the Ethics Committee of Beijing Anzhen Hospital, and the informed consent of all individuals participating in the study or their guardians has been obtained.

Conflicts of Interests The authors declare that they have no competing interests.

References

1. Maaroos, M., et al. (2017). New onset postoperative atrial fibrillation and early anticoagulation after cardiac surgery. *Scand Cardiovasc J, 51*(6), 323–326.
2. Helgadottir, S., et al. (2012). Atrial fibrillation following cardiac surgery: risk analysis and long-term survival. *Journal of Cardiothoracic Surgery, 7*, 87.
3. Hravnak, M., et al. (2002). Resource utilization related to atrial fibrillation after coronary artery bypass grafting. *American Journal of Critical Care, 11*(3), 228–238.
4. Omer, S., et al. (2016). Incidence, Predictors, and Impact of Postoperative Atrial Fibrillation after Coronary Artery Bypass Grafting in Military Veterans. *Texas Heart Institute Journal, 43*(5), 397–403.
5. LaPar, D. J., et al. (2014). Postoperative Atrial Fibrillation Significantly Increases Mortality, Hospital Readmission, and Hospital Costs. *The Annals of Thoracic Surgery, 98*(2), 527–533.
6. Pooria, A., Pourya, A., & Gheini, A. (2020). *Postoperative complications associated with coronary artery bypass graft surgery and their therapeutic interventions. 16*(5): 481-496.
7. Mittal, S., Movsowitz, C., & Steinberg, J. S. (2011). Ambulatory external electrocardiographic monitoring: focus on atrial fibrillation. *Journal of the American College of Cardiology, 58*(17), 1741–1749.
8. Zungsontiporn, N., & Link, M. S. (2018). Newer technologies for detection of atrial fibrillation. *BMJ, 363*, k3946.
9. Dobrev, D., et al. (2019). Postoperative atrial fibrillation: Mechanisms, manifestations and management. *Nature Reviews. Cardiology, 16*(7), 417–436.
10. Barwari, T., Joshi, A., & Mayr, M. (2016). MicroRNAs in Cardiovascular Disease. *Journal of the American College of Cardiology, 68*(23), 2577–2584.
11. Chistiakov, D. A., Orekhov, A. N., & Bobryshev, Y. V. (2016). Cardiac-specific miRNA in cardiogenesis, heart function, and cardiac pathology (with focus on myocardial infarction). *Journal of Molecular and Cellular Cardiology, 94*, 107–121.
12. Shi, K. H., et al. (2013). Role of microRNAs in atrial fibrillation: new insights and perspectives. *Cellular Signalling, 25*(11), 2079–2084.
13. Komal, S., et al. (2019). MicroRNAs: Emerging biomarkers for atrial fibrillation. *Journal of Cardiology, 74*(6), 475–482.
14. Pegtel, D. M., & Gould, S. J. (2019). Exosomes. *Annual Review of Biochemistry, 88*, 487–514.
15. Liu, Y., et al. (2020). Exosomes: From garbage bins to translational medicine. *International Journal of Pharmaceutics, 583*, 119333.
16. Lee, Y. S., & Dutta, A. (2009). MicroRNAs in cancer. *Annual Review of Pathology: Mechanisms of Disease, 4*, 199–227.
17. Condorelli, G., Latronico, M. V., & Cavarretta, E. (2014). microRNAs in cardiovascular diseases: current knowledge and the road ahead. *Journal of the American College of Cardiology, 63*(21), 2177–2187.
18. Chen, X., et al. (2008). Characterization of microRNAs in serum: a novel class of biomarkers for diagnosis of cancer and other diseases. *Cell Research, 18*(10), 997–1006.
19. Zhao, W., Zheng, X. L., & Zhao, S. P. (2015). Exosome and its roles in cardiovascular diseases. *Heart Failure Reviews, 20*(3), 337–348.
20. Mariscalco, G., et al. (2014). Bedside tool for predicting the risk of postoperative atrial fibrillation after cardiac surgery: the POAF score. *Journal of the American Heart Association, 3*(2), e000752.
21. Tran, D. T., et al. (2015). Predicting New-Onset Postoperative Atrial Fibrillation in Cardiac Surgery Patients. *Journal of Cardiothoracic and Vascular Anesthesia, 29*(5), 1117–1126.
22. Mariscalco, G., & Engström, K. G. (2008). Atrial fibrillation after cardiac surgery: risk factors and their temporal relationship in prophylactic drug strategy decision. *International Journal of Cardiology, 129*(3), 354–362.
23. Valadi, H., et al. (2007). Exosome-mediated transfer of mRNAs and microRNAs is a novel mechanism of genetic exchange between cells. *Nature Cell Biology, 9*(6), 654–659.
24. Huang, S., et al. (2021). The Role of Exosomes and Their Cargos in the Mechanism, Diagnosis, and Treatment of Atrial Fibrillation. *Front Cardiovasc Med, 8*, 712828.
25. Song, J. J., et al. (2020). MicroRNA-122 aggravates angiotensin II-mediated apoptosis and autophagy imbalance in rat aortic adventitial fibroblasts via the modulation of SIRT6-elabela-ACE2 signaling. *European Journal of Pharmacology, 883*, 173374.
26. Zhao, Z., et al. (2020). Cholesterol impairs hepatocyte lysosomal function causing M1 polarization of macrophages via exosomal miR-122-5p. *Experimental Cell Research, 387*(1), 111738.
27. Gatfield, D., et al. (2009). Integration of microRNA miR-122 in hepatic circadian gene expression. *Genes & Development, 23*(11), 1313–1326.
28. Zhang, X., & Jing, W. (2018). Upregulation of miR-122 is associated with cardiomyocyte apoptosis in atrial fibrillation. *Molecular Medicine Reports, 18*(2), 1745–1751.
29. González, A., et al. (2018). Myocardial Interstitial Fibrosis in Heart Failure: Biological and Translational Perspectives. *Journal of the American College of Cardiology, 71*(15), 1696–1706.
30. Zhang, Z., et al. (2019). Long non-coding RNA UCA1 relieves cardiomyocytes H9c2 injury aroused by oxygen-glucose deprivation via declining miR-122. *Artif Cells Nanomed Biotechnol, 47*(1), 3492–3499.
31. Cole, J. E., Georgiou, E., & Monaco, C. (2010). The expression and functions of toll-like receptors in atherosclerosis. *Mediators of Inflammation, 2010*, 393946.
32. Hwang, H. J., et al. (2011). Relation of inflammation and left atrial remodeling in atrial fibrillation occurring in early phase of acute myocardial infarction. *International Journal of Cardiology, 146*(1), 28–31.
33. Shao, L., et al. (2014). TLR3 and TLR4 as potential clinically biomarkers of cardiovascular risk in coronary artery disease (CAD) patients. *Heart and Vessels, 29*(5), 690–698.
34. Zhang, P., Shao, L., & Ma, J. (2018). Toll-Like Receptors 2 and 4 Predict New-Onset Atrial Fibrillation in Acute Myocardial Infarction Patients. *International Heart Journal, 59*(1), 64–70.
35. Gurses, K. M., et al. (2016). Monocyte Toll-Like Receptor Expression in Patients With Atrial Fibrillation. *American Journal of Cardiology, 117*(9), 1463–1467.
36. Patel, M. S., & Korotchkina, L. G. (2006). Regulation of the pyruvate dehydrogenase complex. *Biochemical Society Transactions, 34*(Pt 2), 217–222.
37. Jeoung, N. H., & Harris, R. A. (2010). Role of pyruvate dehydrogenase kinase 4 in regulation of blood glucose levels. *Korean Diabetes J, 34*(5), 274–283.
38. Pathak, R. K., et al. (2015). Long-Term Effect of Goal-Directed Weight Management in an Atrial Fibrillation Cohort: A Long-Term Follow-Up Study (LEGACY). *Journal of the American College of Cardiology, 65*(20), 2159–2169.
39. Abed, H. S., et al. (2013). Effect of weight reduction and cardiometabolic risk factor management on symptom burden and severity in patients with atrial fibrillation: a randomized clinical trial. *JAMA, 310*(19), 2050–2060.

40. Raman, K., et al. (2016). Whole Blood Gene Expression Differentiates between Atrial Fibrillation and Sinus Rhythm after Cardioversion. *PLoS ONE, 11*(6), e0157550.
41. Nagpal, N., & Kulshreshtha, R. (2014). miR-191: an emerging player in disease biology. *Frontiers in Genetics, 5*, 99.
42. Baglio, S. R., et al. (2015). Human bone marrow- and adipose-mesenchymal stem cells secrete exosomes enriched in distinctive miRNA and tRNA species. *Stem Cell Research & Therapy, 6*(1), 127.
43. Wei, C., et al. (2013). Circulating miRNAs as potential marker for pulmonary hypertension. *PLoS ONE, 8*(5), e64396.
44. Qi, M., et al. (2020). MiR-181a-5p is involved in the cardiomyocytes apoptosis induced by hypoxia-reoxygenation through regulating SIRT1. *Bioscience, Biotechnology, and Biochemistry, 84*(7), 1353–1361.
45. Chen, A., et al. (2020). Inhibition of miR-155-5p attenuates the valvular damage induced by rheumatic heart disease. *International Journal of Molecular Medicine, 45*(2), 429–440.
46. Neiburga, K.D., et al. (2021). *Vascular Tissue Specific miRNA Profiles Reveal Novel Correlations with Risk Factors in Coronary Artery Disease.* Biomolecules, *11*(11).